

PVP-I reduces LPS-induced airway inflammation by blocking TLR4 signaling in airway epithelial cells

Seung Hoon Lee¹, Sun-Hee Yeon¹, Seung-Hyeon Choi¹, Soo-Kyoung Park¹, Mi Ra Choi¹, and Yong-Min Kim¹

¹Chungnam National University School of Medicine

April 05, 2024

Abstract

Background: Povidone-iodine (PVP-I) is an antiseptic and a disinfectant with broad-spectrum antimicrobial activity against various pathogens. However, it is unclear whether PVP-I nasal instillation can suppress mucosal inflammation in non-eosinophilic chronic rhinosinusitis (CRS) mice. **Objective:** This study aimed to explore the anti-inflammatory effects and underlying molecular mechanism of PVP-I on lipopolysaccharide-stimulated airway epithelial cells and investigate whether nasal instillation of PVP-I can suppress mucosal inflammation in non-eosinophilic CRS mice. **Methods:** Inflammation-related molecules in the nasal epithelial cells and non-eosinophilic CRS mice were measured by enzyme-linked immunosorbent assay, western blotting, quantitative real-time polymerase chain reaction, immunoprecipitation, and histopathological analysis (hematoxylin and eosin staining, immunohistochemistry, and periodic acid-schiff staining). **Results:** PVP-I blocked expressions of various inflammation-related molecules, such as NLRP3, NF- κ B-p65, caspase-1, and IL-1 β ; induced translocation of NF- κ B to the nucleus; and promoted assembly of NLRP3/ASC complexes in the nasal epithelial cells and non-eosinophilic CRS mice. Notably, PVP-I strongly blocked the receptor interaction of TLR4 and MyD88 in the epithelial cells of nasal mucosa. **Conclusion:** We demonstrated that PVP-I significantly attenuated inflammatory molecules and cytokines via blocking the formation of TLR4 and MyD88 complexes during LPS-induced mucosal inflammation in non-eosinophilic CRS.

INTRODUCTION

Chronic rhinosinusitis (CRS) is a persistent inflammatory disease of the nasal and paranasal sinuses mucosa.¹ CRS is a heterogeneous disorder with distinct pathophysiologic mechanisms, and evidence from several studies has revealed different endotypes.²⁻⁴ The selective expression of type 1, 2, or 3 immune responses is associated with increasing CRS heterogeneity.⁵⁻⁸ An endotype of CRS with prominent type 2 immune responses is associated with eosinophilic infiltration into sinonasal mucosa and can benefit from treatment with systemic steroids and biologics, whereas non-eosinophilic CRS shows resistance to these therapy.⁹⁻¹²

Nucleotide-binding oligomerization domain-like receptor family pyrin domain-containing 3 (NLRP3) could combine with the Apoptosis-associated speck-like protein containing a caspase recruitment domain (ASC) and the pro-caspase-1 to compose the NLRP3 inflammasomes¹³. NLRP3 inflammasomes play essential roles in the innate and adaptive immune responses serving as a pattern-recognition receptor and a trigger for caspase-1 activation and the maturation of IL-1 β and IL-18.^{14,15}

The NLRP3 and its downstream IL-1 β were identified as potent inducers of neutrophilic inflammation in various inflammatory diseases.^{16,17} Previous studies showed that NLRP3 was highly expressed in nasal polyps (NPs) from subjects with CRSwNP, and significantly correlated with neutrophilic nasal polyps.^{18,19} Wei et al. reported that macrophages and epithelial cells were the primary sources of NLRP3 in the polyp tissues.¹⁹

Povidone-iodine (PVP-I) is an antiseptic and a disinfectant with broad-spectrum antimicrobial activity. It has been used as a topical treatment and surgical scrubs for several decades.²⁰⁻²² PVP-I consists of a complex

of povidone, hydrogen iodide, and elemental iodine.²³

PVP-I is effective in reducing edema or tissue inflammation and promoting wound healing, as well as eradication of most pathogens.^{24,25} Here, PVP-I was more effective in non-eosinophilic CRS than its eosinophilic counterpart in terms of decreasing sinus discharge and improving olfaction and up to a 17% reduction in serum inflammatory markers was measured post-PVP-I rinsing.²⁶

Although non-eosinophilic CRS has been associated with various bacterial infections, refractory CRS has been revealed to be closely associated with Gram-negative bacterial infection, and the endotoxins and LPS released by Gram-negative bacteria are considered as important pathogenic mechanisms.^{27,28} While endotoxin may be a noninfectious inflammatory factor, it can regulate the release of inflammatory mediators, resulting in CRS.^{27,29}

Here, we explore the anti-inflammatory effects and the underlying molecular mechanism of PVP-I on LPS-stimulated airway epithelial cells and investigate whether nasal instillation of PVP-I can suppress mucosal inflammation in non-eosinophilic CRS mice.

METHODS

Chemicals

Adenosine triphosphate (ATP, A2383), lipopolysaccharide (LPS, L2630), and Poly(vinylpyrrolidone)-iodine complex (PVP-I, PVP1) were purchased from Sigma (St. Louis, MO, USA).

Cell cultures, human nasal airway epithelial primary cells

A549 cells (human lung airway epithelial) and RPMI 2650 cells (airway epithelial, human nasal septum) were cultured at 37°C, and 5% CO₂ in RPMI medium (Gibco, Gaithersburg, MD USA) supplemented with 10% FBS (Gibco), 100 U/mL penicillin, and 100 µg/mL streptomycin (Gibco). For preparation, primary human nasal epithelial cells (pHNECs, n=19) were derived from patients undergoing elective endoscopic sinus surgery and were provided by the Department of Otorhinolaryngology-Head and Neck Surgery, Chungnam National University Hospital. The pHNECs were incubated overnight in 1% Dispase II (Roche, Belmont, CA, USA) at 4°C, digested with 0.25% Trypsin-EDTA (Gibco) for 15 min at 37°C, and neutralized with 10% FBS. The digested tissue was passed through a 70 µm cell strainer (SPL, Pocheon, Korea) to remove the undigested tissue for collecting pHNECs and washed twice with RPMI medium. Then, the tube was centrifuged at 1,300 rpm for 5 min. The obtained pHNECs were cultured in airway epithelial cell growth media (PromoCell, Heidelberg, Germany) supplemented with a mixture of amphotericin B (25 µg/mL), penicillin G (10,000 U/mL), and streptomycin (10,000 µg/mL). The cells were placed in a humidified chamber and incubated at 37°C, 5% CO₂, and 95% air for two weeks. The second cell passage provided all of the cells used in this study. The cells were stimulated with LPS (1000 ng/mL) and ATP (5 mM) for 24 h, and PVP-I (0.1%) was additionally added to the cell culture for 1 h after LPS or ATP stimulation or both.

Animal study

Animal experiments were conducted using seven-weeks-old male C57BL/6 mice with 18–20 g body weight (Orient Bio Inc., Seungnam, Republic of Korea). This study protocol was approved by the Chungnam National University's Institutional Animal Care and Use Committees (CNUH-20018). The mice were maintained under specific-pathogen-free conditions, consisting of a 12-h light/dark cycle, a temperature of 18°C–23°C, and humidity of 50%–60%. Food and water were available *ad libitum*. After one week of acclimation in an animal facility, mice were divided into four groups: control, LPS group, LPS + intraperitoneal (IP) of dexamethasone (DEX) at 1 mg/kg, and LPS + intranasal (IN) of PVP-I at 0.1%. LPS was dissolved in Dulbecco's phosphate-buffered saline (DPBS) and injected intranasally (10 µg/kg) in 20-µL DPBS with a 10-µL pipette three times a week for three consecutive months. Then, PVP-I was dissolved in DPBS and administered intranasally once per day for seven days, and DEX administered intraperitoneally three times per day for seven days.

The animals were sacrificed seven days after sensitization with DEX and PVP-I treatment (See Figure 5A for a timeline). After partial tracheal resection under deep anesthesia, a micropipette was inserted into the posterior choana through the tracheal opening in the upper airway direction. Each nasal lavage fluid (NLF) was gently perfused with 200 μ L DPBS, and fluid from both nostrils was collected and centrifuged for IL-1 β enzyme-linked immunosorbent assay (ELISA). The head of each mouse was removed and fixed in 4% paraformaldehyde. Serial 4 μ M thick sections were cut on a paraffin microtome designed for histological analysis using H&E, IHC, and PAS. The nasal mucosa tissue was meticulously excised using a small curet and micro-forceps. The harvested nasal mucosa was immediately soaked in T-PER Tissue lysis buffer for immunoblot analysis.

Cytotoxicity measures

A549 and RPMI2650 cells were plated as stated above in clear 96-well plates. After incubation time, the ATP, LPS, and PVP-I were treated in varying concentrations and incubated for another 24 h. After completion, the cell suspension was discarded, and 1 mg/mL MTT solution was added and incubated for 4 h, and then DMSO was added. The absorbance was then taken at 570 nm. The absorbance of each well was measured using a spectrophotometer (Versamax microplate reader, Molecular Device, Sunnyvale, CA, USA) at a wavelength of 570 nm, and expressed as a percentage of the control.

Immunoblot

The protein samples from airway epithelial cells (A549 and RPMI2650 cells) were prepared in radio immunoprecipitation assay (RIPA) lysis buffer (5 mM sodium fluoride, 10 μ g/mL phenylmethylsulfonyl fluoride, and 1 mM sodium vanadate) containing a protease inhibitor cocktail (Roche, Mannheim, Germany). Mouse mucosa tissue protein samples were prepared in T-PER Tissue lysis buffer (78510, Thermo Fisher Scientific, T-PER Tissue lysis Protein Extraction Reagent). All samples were separated on 12% SDS-polyacrylamide gels (SDS-PAGE) and then transferred to PVDF membranes, blocked with 5% w/v nonfat dry milk in PBS containing 0.5% Tween-20. The primary antibodies used were actin (CS-8457P, Cell Signaling, Danvers, MA, USA), caspase-1 (MA5-32909, Thermo Fisher Scientific, Waltham, MA, USA), IL-1 β (GTX74034, genetex, USA), I κ B- α (4814P, Cell Signaling), lamin B1 (AB65986, abcam, United Kingdom), NF- κ B-p65 (8242S, Cell Signaling), NLRP3 (AG-20B-0014, Adipogen, SA, Switzerland), and tubulin (T8023, Sigma).

Histopathology

Cells were fixed by incubation with 4% paraformaldehyde at room temperature for 30 min. Fixed cells were rinsed in PBS, treated with 0.5% bovine serum albumin for 30 min, and then incubated overnight at 4°C with rabbit anti-NLRP3, ASC, NF- κ B-p65, and - IL-1 β antibodies (each diluted 1:500). They were then incubated for 2 h with Alexa 488 and 594 fluor-conjugated secondary antibody (dilution 1:2000). The cells were finally washed in PBS and mounted using Vectashield mounting-medium containing 4'6-diamidino-2-phenylindole. Immunofluorescent images were captured using a microscope (Olympus Microscope System BX51; Olympus, Tokyo, Japan).

For H&E analysis, each mouse's head was removed and fixed in 4% paraformaldehyde. Serial 4 μ M thick sections were cut on a paraffin microtome designed for histological analysis using H&E.

For immunohistochemistry, paraffin sections were dewaxed, and incubated with 3% hydrogen peroxide at room temperature for 10 min to inactivate endogenous peroxidase. The sections were placed into an antigen retrieval solution (0.01 M citrate), repaired using a pressure cooker at 100°C for 5 min and cooled to room temperature before washing five times with PBS for 5 min each. Sections were subsequently blocked with 1% bovine serum albumin at room temperature for 60 min and incubated overnight at 4°C with anti-mouse TLR4 monoclonal antibody at a dilution of 1:100. After washing, the sections were incubated with horse-radish peroxidase (HRP) at 37degC in a humidified chamber for 60 min and subsequently washed five times with PBS for 5 min each. The sections were developed with 3'-Diaminobenzidine (DAB) and washed immediately with running water when brown particles appeared in the cytoplasm to terminate the reaction. The sections were secondarily stained with hematoxylin for 1 min.

For periodic acid-schiff staining (PAS), at room temperature, paraffin-embedded tissue sections were serially dehydrated in xylene and ethanol. Then, sections were stained with PAS. Slides were incubated with 0.5% periodic acid solution for 5 min, then stained with Schiff's reagent for 15 min, followed by counterstaining with hematoxylin solution for 1 min.

Immunoprecipitation

Protein samples from airway epithelial cell extracts and mouse mucosa tissue cell extracts (500 µg protein) were immunoprecipitated by incubation with anti-TLR4 or MyD88 antibody (25 µg) overnight at 4°C, followed by incubation with protein G-agarose bead (40 µL of a 1:1 slurry) for 1 h at room temperature. Immune complexes were washed five times with a RIPA buffer, boiled for 5 min in a Laemmli sample buffer, and analyzed by SDS-PAGE and immunoblotting with the indicated antibodies. The immunoprecipitation antibodies used were TLR4 (SC-293072, Santa Cruz Biotechnology, Santa Cruz, CA, USA) and MyD88 (SC-74532, Santa Cruz Biotechnology).

Proteome profiler antibody array analysis

The protein from airway epithelial cells and pHNECs was extracted using a RIPA lysis buffer. Proteome Profiler Human XL Cytokine Array Kit (#ARY022B) is membrane-based sandwich immunoassay. Following manufacturer recommendations, each membrane was incubated with 100 µL of pooled plasma overnight at 4°C. Captured plasma proteins were detected with biotinylated detection antibodies and afterward, visualized with Streptavidin-HRP and chemiluminescent detection reagents. A signal was produced at each capture spot, proportionally with the amount of the protein-bound. The signal produced is proportional to the amount of analyte bound. The bands' intensities were analyzed using Quick Spots Image Analysis Software (Western Vision Software, <http://www.wvision.com/QuickSpots.html>).

Real-time quantitative polymerase chain reactions

According to the manufacturer's instructions, total RNAs from the cells and mice nasal mucosa were extracted using TRIzol reagent (Thermo Fisher Scientific). AccuPower RT PreMix (Bioneer, Daejeon, Korea) was used for complementary DNA (cDNA) synthesis according to the manufacturer's instructions. The obtained cDNA was amplified with specific primers (Table 1). Polymerase chain reaction (PCR) was performed for cDNA synthesis using a T100 Thermal Cycler (Bio-Rad Laboratories, USA). The mRNA expression was analyzed using a CFX Connect Real-Time PCR Detection System (Bio-Rad Laboratories, USA) with PowerUp SYBR Green Master Mix (Applied Biosystems, USA). All PCR assays were performed in triplicate. The relative gene expression was analyzed using the $2^{-[Ct]}$ method. The details of the primers are shown in Table 1.

IL-1β Ενζψμε-Αινκεδ Ιμμυνοσορβεντ Ασσαψ

The supernatants from cultured A549, RPMI2650, and pHNECs were collected. Protein levels of IL-1β in the supernatants were detected using ELISA kits (SLB50, R & R&D Systems, Minneapolis, MN, USA). Assay diluent was added to each well with the standard and samples, and the wells were covered using an adhesive strip and incubated at room temperature. Each well was aspirated and washed as the complete removal of the liquid at each step is essential for best performance. Conjugate was added to each well, and the above steps were repeated. Plates were washed with a wash buffer, and substrate solution was added to each well and incubated for 30 min at room temperature. Notably, the procedure requires the samples to be protected from light. Once 1 mol/L sulfuric acid was added, the substrate reaction is halted, and the extinction was measured at a wavelength of 450 nm using a multi-plate ELISA reader. According to the manufacturer's instructions, in mice NLF, IL-1β levels were detected using the ELISA kits (SMLB00C, R&D Systems).

Isolation of cytosolic and nuclear fractions

Nuclear protein extracts from A549 and RPMI2650 cells were prepared using the NE-PER kit (Thermo Fisher Scientific, USA) according to the manufacturer's instructions. After that, nuclear proteins (the supernatant)

were used immediately or stored at -80°C .

Statistical analysis

Data are expressed as mean \pm standard error (SEM). The data were analyzed via a one-way analysis of variance (ANOVA) and post-hoc multiple variation comparisons (Tukey's HSD test). All data were analyzed using GraphPad Prism v.5.10 software (GraphPad Software Inc., San Diego, CA, USA). Statistical comparisons between the different treatments were performed using one-way ANOVA with the Tukey multiple comparison post-test. P -values of $<.05$ were considered as statistically significant.

RESULTS

Π*Π-I συπρεσς ΝΛΡΠ3- ανδ ΝΦ-κΒ-δεπενδεντ ινφλαμματορψ πατηωαψς ιν αιρωαψ επιτηελιαλ ςελλς

LPS, ATP, and PVP-I concentrations were selected up to 1000 ng/mL, 5 mM, and 0.1% for the following experiments, respectively (Fig. S1A). Protein expression of NLRP3 were elevated in the LPS and ATP (LPS/ATP) treated cells compared with cells treated with LPS or ATP alone (Fig. S1B). Expressions of NLRP3 mRNA were also significantly elevated in LPS/ATP treated cells compared with cells treated with each alone (Fig. S1C).

Protein and mRNA expression of NLRP3 induced by LPS/ATP was significantly decreased by PVP-I treatment in airway epithelial cells (Fig. 1A and B). NLRP3 inflammasome-associated molecules were also evaluated in these airway epithelial cells, and expression of NF- κ B-p65, caspase-1, and IL-1 β were strongly inhibited by PVP-I treatment in both protein and mRNA levels (Fig. 1C and D). Treatment of LPS/ATP allowed NF- κ B-p65 translocation to the nucleus and I κ B- α degradation in the cytosol, and these phenomena were reversed by treatment of PVP-I (Fig. 1E). Immunofluorescence analysis also showed that LPS/ATP-induced NF- κ B-p65 translocation to the nucleus was inhibited by PVP-I treatment in airway epithelial cells (Fig.1F). NLRP3/ASC assemblies in the cytoplasm were also induced by LPS/ATP treatment, and were inhibited by PVP-I treatment in airway epithelial cells (Fig. 1G).

LPS/ATP-induced expressions of NLRP3, NF- κ B-p65, caspase-1, and IL-1 β , and NLRP3/ASC assemblies were suppressed by PVP-I treatment in pHNECs (Fig. 2B–D). These results indicated that PVP-I treatment could inhibit the activation of NLRP3 inflammasome and associated molecules in airway epithelial cells.

PVP-I inhibits LPS/ATP-induced cytokine production in airway epithelial cells

LPS/ATP-induced production of IL-1 β was markedly reduced by PVP-I treatment (Fig. 3A). PVP-I treatment reduced the NF- κ B signaling related cytokines (APoA1, Ang-1, BAFF, CD40L, EGF, Fas L, GM-CSF, GRO α , CD54L, IFN- γ , IL-1 α , IL-1ra, IL-4, IL-6, IL-8, IL-10, IL-12p70, IL-17A, IL-23, IP-10, MCP1, M-CSF, MMP9, TFF3, TNF- α , VESF, and VCAM-1) induced by LPS/ATP stimulation in pHNECs (Fig. 3B and S3). Also, LPS/ATP-induced IL-1 β cytokine production (red box in Fig. 3B) was significantly decreased by PVP-I treatment in pHNECs (Fig. 3B and C). These results demonstrated that PVP-I strongly inhibits the production of pro-inflammatory or inflammatory cytokines, which inflammatory mediator induces.

PVP-I suppresses LPS/ATP-induced inflammatory response by blocking TLR4 signaling

The binding of TLR4 and MyD88 are crucial for signaling inflammatory response.⁴¹ The formation of TLR4 and MyD88 was increased after LPS/ATP stimulation, and treatment of PVP-I inhibited the intensity of the TLR4 band immunoprecipitated with an anti-MyD88 protein (Fig. 4A and B). The reverse immunoprecipitation of MyD88 with TLR4 antibody also showed blocking of complex formation after PVP-I treatment (Fig. 4A and B). This result indicated that PVP-I could inhibit TLR4/MyD88 complex formation, which is induced by LPS/ATP stimulation.

PVP-I inhibits mucosal inflammation in mice with CRS

Mucosal thickness (H&E stain, Fig. 5B) and the number of goblet cells (PAS stain, Fig. 5C) were significantly decreased in the groups of dexamethasone (LPS + DEX) or PVP-I treatment (LPS + PVP-I) compared

with the PBS treatment group (LPS + PBS). TLR4 expression among groups was significantly higher in the LPS + PBS group compared with other groups (Fig. 5D). TLR4/MyD88 complex formation stimulated with LPS was inhibited by PVP-I or dexamethasone treatment in the nasal mucosa (Fig. 5E).

NF- κ B-p65, caspase-1, and IL-1 β were significantly inhibited by PVP-I treatment (LPS + PVP-I) or dexamethasone (LPS + DEX) (Fig. 6A and B). In addition, IL-1 β production in NLF was significantly decreased in the mice treated with dexamethasone or PVP-I (Fig. 6C). The mRNA expressions of TNF- α , IFN- γ , IL-4, and IL-17 were significantly higher in LPS-induced CRS mice (LPS + PBS) compared with control mice, and these cytokines were significantly decreased by PVP-I (LPS + PVP-I) and dexamethasone (LPS + DEX) treatment (Fig. 6D). These results indicated that topical instillation of PVP-I in mice alleviates mucosal inflammation of LPS-induced CRS mice.

DISCUSSION

Inflammatory responses exert their effect on cells mainly through the NF- κ B signaling.¹⁸ We found that PVP-I inhibited several molecules' expression in this signaling, such as NLRP3, NF- κ B-p65, caspase-1, and IL-1 β in LPS/ATP-induced airway epithelial cells and pHNECs. (Figs. 1 and 2). Previous studies have reported anti-inflammatory mimic effects of PVP-I.²³⁻²⁶ However, the underlying molecular mechanisms of PVP-I on anti-inflammatory effects were not revealed. To our knowledge, this is the first study that evaluates the underlying mechanisms of PVP-I on inflammation in airway epithelial cells.

We tried verifying the anti-inflammatory effect of PVP-I using the NLRP3 inflammasome signal model *in vitro*. Recent studies have shown that NLRP3 inflammasome plays a pivotal role in various diseases, such as CRS, asthma, obstructive pulmonary disease, inflammatory bowel disease, metabolic disorders, multiple sclerosis, and other auto-immune and auto-inflammatory diseases.³⁴⁻³⁸ Our results demonstrated that PVP-I effectively suppressed NLRP3 inflammasome-associated molecules and cytokines, activated by LPS/ATP stimulation.

To inhibit the inflammatory signal inside airway epithelial cells, free iodine may be able to enter the cytosol through the cell membrane. This allowed the destruction of cellular components, including enzymes essential to survive. Because 0.1% of PVP-I did not show cellular toxicity, other mechanisms may be involved in suppressing cellular signaling molecules and inflammatory cytokines in this study. Our findings suggest that PVP-I could inhibit the inflammatory response via TLR4 and MyD88 complex formation. Free iodine released by PVP-I is a strong oxidizing agent, and there is a possibility that free iodine destroys some parts of TLR4 and disturbs joining with MyD88; thus, blocking signal transmission. Indeed, TLR4 induced by LPS was suppressed by PVP-I treatment in airway epithelial cells (Fig. 4A and B).

A study indicated that NLRP3 inflammasome is more associated with non-eosinophilic CRS. Because the PVP-I target was thought to be TLR4 *in vitro*, expressions of TLR4 and TLR4-related signal molecules were evaluated in mice, and these were decreased in PVP-I treated mice. Interestingly, IL-4 expression in mice nasal mucosa was also suppressed after PVP-I treatment. Future studies investigating PVP-I-induced suppression of PRR and other surface receptors are required.

In NPs of patients with CRS, several types of cytokine expression are involved with inflammation.⁷ Our results showed that PVP-I inhibited the inflammation-induced IL-1 β secretion, and 27 cytokines in airway epithelial cell lines and primary cultured cells from nasal polyp patients (Fig. 3 and S3). In the pathogenesis of CRSwNP in Asian patients, NF- κ B-associated inflammatory cytokines are a key factor and thought of as a therapeutic target.⁴⁵ This finding suggests that the PVP-I strongly inhibited inflammation signaling through NF- κ B related molecule, such as IL-1 β , and PVP-I may be used as a possible therapeutic remedy in CRS, especially non-eosinophilic CRS.

The therapeutic effects of PVP-I were similar to those of dexamethasone in our study. Anti-inflammatory effects of dexamethasone have been well described.⁵⁰ Dexamethasone showed its effect by inhibiting NF- κ B and other inflammatory transcription factors and promoting anti-inflammatory genes.⁵¹ Although the effects of dexamethasone were similar to those of PVP-I in this study, these drugs' target and route were

quite different. Generally, the side effect of PVP-I is less serious than those of dexamethasone even when used long term.

Here, PVP-I was the first used to study an anti-inflammatory response by inhibiting the goblet cells in the NPs mouse models' mucosa tissue. In this study, PVP-I ameliorated goblet cell hyperplasia in neutrophilic CRS mice. Although we did not conduct an animal study in the eosinophilic mice model, PVP-I may effectively suppress mucosal inflammation, including goblet cell hyperplasia because PVP-I blocked the inflammation-related cytokines, such as TNF- α , IL-1 β , and IL-4 in mucosa tissue of NPs mice models (Fig. 6A and B). Future studies are required to verify these effects in the eosinophilic CRS model. A study also demonstrated that diluted topical PVP-I rinses showed notable symptom improvement, especially discharge score in recalcitrant CRS, without affecting thyroid function, mucociliary clearance, or olfaction.⁵⁷

In summary, we demonstrated that PVP-I significantly attenuated inflammatory molecules and cytokines via blocking the formation of TLR4 and MyD88 complexes in the LPS-induced mucosal inflammation in non-eosinophilic CRS. We believe PVP-I could modulate critical inflammatory signals, and the need to study PVP-I-related signal inhibition on the cell surface receptors or molecules, such as pattern-recognition receptors, in the future. We also believe that ACE2 (angiotensin-converting enzyme 2) and TMPRSS2 (transmembrane protease serine subtype 2) could be a target for PVP-I rinses of the upper airway.

FIGURE LEGEND

Figure 1. LPS plus ATP activates NLRP3 inflammasome response in airway epithelial cells.

Treatment of airway epithelial cells with LPS and ATP with or without the PVP-I inhibited the induction of NLRP3 inflammasome protein, as shown **(A)** immunoblot and **(B)** qRT-PCR. Cells were stimulated with LPS and ATP for 24 h, and PVP-I (0.1%) was additionally added to the cell culture for 1 h (to produce an inflammation environment) after LPS and/or ATP stimulation. Statistical significance: *P <.05 and **P <.01 compared with the control group; #P <.05 and ##P <.01 compared with the LPS/ATP group. **(C and D)** Protein and mRNA expression of NF- κ B-p65, caspase-1 and IL-1 β in airway epithelial cells treated with LPS, ATP with or without PVP-I, as shown by immune blot and qRT-PCR. Statistical significance: *P <.05 and **P <.01 compared with the control group; #P <.05, ##P <.01 and ###P <.01 compared with the LPS/ATP group. **(E)** Cytosolic and nuclear extracts were analyzed by immune blot with indicated antibodies for NF- κ B-p65 and I κ B- α . Anti-Lamin B and anti- α -tubulin antibodies were used as loading controls for the nucleus and cytosol, respectively. **(F)** Representative Immunofluorescence of NF- κ B-p65 translocation to nucleus (green) and DAPI (blue) localization in airway epithelial cells. The scale bar indicates 100 μ m. **(G)** Immunofluorescence for NLRP3 (red) and ASC (green) co-localization in airway epithelial cells. The scale bar indicates 100 μ m.

Figure 2. Alteration of inflammation molecules in primary cultured cells from nasal polyp patients.

(A) Optical microscope of cell viability in the human nasal epithelial primary cells (pHNECs) from nasal polyp patients. Primary cultured cells from nasal polyp patients were treated with LPS (1000 ng/mL), ATP (5 mM) and PVP-I (0.1%) for 24 h. Representative photomicrographs of cell morphology was measured using an optical microscope. **(B and C)** mRNA and protein expression of NLRP3, NF- κ B-p65, caspase-1 and IL-1 β in pHNECs treated with LPS, ATP with or without PVP-I, as shown by qRT-PCR and immunoblot. Statistical significance: *P <.05, **P <.01 and ***P <.001 compared with the control group; #P <.05 compared with the LPS/ATP group. **(D)** Immunofluorescence for NLRP3 (red) and ASC (green) co-localization in pHNECs. The scale bar indicates 100 μ m.

Figure 3. Profiling proteins by inflammation response in airway epithelial cells.

Inhibition of LPS and ATP-induced IL-1 β secretion by PVP-I. Airway epithelial cells were treated with PVP-I (0.1%) for 1 h after LPS (1000 ng/mL) and ATP (5 mM) treatment. **(A)** After 24 h-incubation, the airway epithelial cell culture medium was assayed using an ELISA for IL-1 β . Statistical significance: *P <.05 and **P <.01 compared with the control group; ##P <.01 compared with the LPS/ATP group. **(B)** After 24

h-induction, the pHNECs were subjected to cytokine antibody array assay. Each proteins represented by duplicate spots in the respective membrane. IL-1 β protein is boxed in red. **(C)**Data were analyzed using the Quick Spots Image Analysis Software. Statistical significance: ***P <.001 compared with the control group; ##P <.01 compared with the LPS/ATP group.

Figure 4. PVP-I inhibits TLR4 and MyD88 interaction by inflammation response

Airway epithelial cells were pre-treated with LPS (1000 ng/mL) and ATP (5 mM) for 60 min and then exposed to 0.1% PVP-I for 24 h. Cells lysate were immunoprecipitation with anti- MyD88 and TLR4 antibody, and then immunoprecipitated proteins were detected using anti-TLR4 and anti-MyD88 antibodies. The pHNECs had the same experimental methods as the airway epithelial cells. PVP-I was found to inhibit the interaction with TLR4 and MyD88 complex formation. Actin was used as a control for input.

Figure 5. PVP-I inhibits inflammation in LPS-stimulated mice.

(A) Nasal polyps mouse models protocol. Mice were assigned to 4 groups and administered saline or PVP-I at doses of 0.1% intra-nasally for on 7 days after LPS administration (intra-nasal) for 12 weeks.

Nasal polyps mouse models protocol. Mice were assigned to 4 groups and administered PVP-I at doses of 0.1% intra-nasally or DEX at doses of 1 mg/kg intraperitoneally for on 7 days after 10 μ g LPS intra-nasally for 12 weeks. **(B)** Representative hematoxylin and eosin staining to demonstrate nasal mucosa tissue. Statistical significance: *P <.05 compared with the control group; #P <.05 compared with the LPS+PBS group; §P <.05 compared with the LPS+DEX group. **(C)** Goblet cells increased in the epithelium with PAS staining upon LPS administration. In the epithelium, number of goblet cells of the LPS administration group was more than in the CON group, and was further inhibited in the PVP-I treatment group. Statistical significance: **P <.01 compared with the control group; #P <.05 compared with the LPS+PBS group; §P <.05 compared with the LPS+DEX group. **(D)** Immunohistochemistry showing the TLR4 and MyD88 in the nasal mucosa of mice in each group. Statistical significance: *P <.05 compared with the control group; §P <.05 compared with the LPS+DEX group. **(E)** Cells lysate in murine nasal mucosa tissue were immunoprecipitation with anti- MyD88 and TLR4 antibody, and then immunoprecipitated proteins were detected using anti-TLR4 and anti-MyD88 antibodies. PVP-I was found to inhibit the TLR4 and MyD88 complex formation. Actin was used as a control for input.

Figure 6. PVP-I inhibits TLR4 and MyD88 complex formation in nasal polyps mouse model.

(A) Bar graphs represent the relative expression of cytokines. Statistical significance: *P <.05, **P <.01 and ***P <.001 compared with the control group; #P <.05, ##P <.01 and ###P <.001 compared with the LPS+PBS group; §P <.05, §§P <.01 and §§§P <.001 compared with the LPS+DEX group. **(B)** The expression of NLRP3, NF- κ B-p65, caspase-1 and IL-1 β were measured using an immunoblot in murine nasal mucosa tissues. Actin protein was used as a loading control. **(C)** Production of IL-1 β in the nasal lavage fluid (NLF) were measured using the ELISA assay. Statistical significance: ***P <.001 compared with the control group; #P <.05 compared with the LPS+PBS group; §P <.05 compared with the LPS+DEX group.

Table 1. Details of the oligonucleotide sequences for qRT-PCR

Oligonucleotides			
Gene	5'→	Human	Mouse
NLRP3	Forward	GGACTGAAGCACCTGTTGTGCA	TCACAACTCGCCC AAGGAGGAA
	Reverse	TCCTGAGTCTCCCAAGGCATTC	AAGAGACCACGGCAGAAAGCTAG
Caspase-1	Forward	GCTGAGGTTGACATCACAGGCA	GGCACATTTCCAGGACTGACTG
	Reverse	TGCTGTCAGAGGCTTTGTGCTC	GCAAGACGTGTACGAGTGGTTG
IL-1β	Forward	CCACAGACCTTCCAGGAGAATG	TGGACCTTCCAGGATGAGGACA
	Reverse	GTGCAGTTCAGTGATCGTACAGG	GTTTCATCTCGGAGCCTGTAGTG
NF-κB-p65	Forward	TGAACCGAAACTCTGGCAGCTG	TCCTGTTCGAGTCTCCATGCAG
	Reverse	CATCAGCTTGGCAAAGGAGCC	GGTCTCATAGGTCCTTTTGCCG
IL-4	Forward	CCGTAACAGACATCTTTGCTGCC	ATCATCGGCATTTTAACGAGGTC
	Reverse	GAGTGTCCCTTCATGTTGGCT	ACCTTGAAGCCCTACAGACGA
IL-17	Forward	CGGACTGTGATGGTCAACCTGA	CAGACTACCTCAACCGTTCCAC
	Reverse	GCACCTTGCCTCCAGATCACA	TCCAGCTTTCCCTCCGCATTGA
TNF-α	Forward	CTCTTCTGCCTGCTGCACCTTG	GGTGCCTATGCTCAGCCCTCTT
	Reverse	ATGGGCTACAGGCTTGTCACTC	GCCATAGAAGCTGATGAGAGGGAG
IFN-γ	Forward	GAGTGTGGAGACCATCAAGGAAG	CAGCAACAGCAAGGCCAAAAAGG
	Reverse	TGCTTTCGCTGGACATTCAGTC	TTTCCGCTTCTGAGGCTGGAT

Supplementary Figure Legends

Supplementary E1. Cell viability of LPS, ATP and PVP-I in airway epithelial cells.

Effect of LPS, ATP and PVP-I on airway epithelial cells (A549, RPMI2650 cells). **(A)** After serum starvation, cells were treated with various concentration of LPS, ATP and PVP-I for 24 h. The viability of the cells were measured by the MTT assay. **(B and C)** LPS/ATP induced changes of NLRP3 protein and mRNA levels in airway epithelial cells. Cells were treated with LPS 1000 ng/mL and ATP 5 mM for 24 h. Statistical significance: *P <.05 compared with the control group; ##P <.01 compared with the LPS group; §§<.01, §§§<.001 compared with the ATP group.

Supplementary E2. Localization of NLRP3 in airway epithelial cells.

Airway epithelial cells were treated with LPS (1000 ng/mL) and ATP (5 mM) for 60 min. **(A)** After 24 h-indubation, immunofluorescence for NLRP3 (red) localization in A549 cells. **(B)** After 24 h-indubation, immunofluorescence for NLRP3 (red) localization in RPMI2650 cells. The scale bar indicates 100 μm.

Συμπλεμενταρψ Ε3. Ινφλαμματορψ ςψτοκινες ωιτη ΝΦ-κΒ ιν πΗΝΕ΄ς.

pHNECs were treated with PVP-I (0.1%) for 1 h after LPS (1000 ng/mL) and ATP (5 mM) treatment. After 24 h-incubation, the pHNECs culture medium was assayed using an ELISA for inflammarty cytokines-related NF-κB signaling. Densitometric ratios of the array showed differences in the inflammation cytokines.

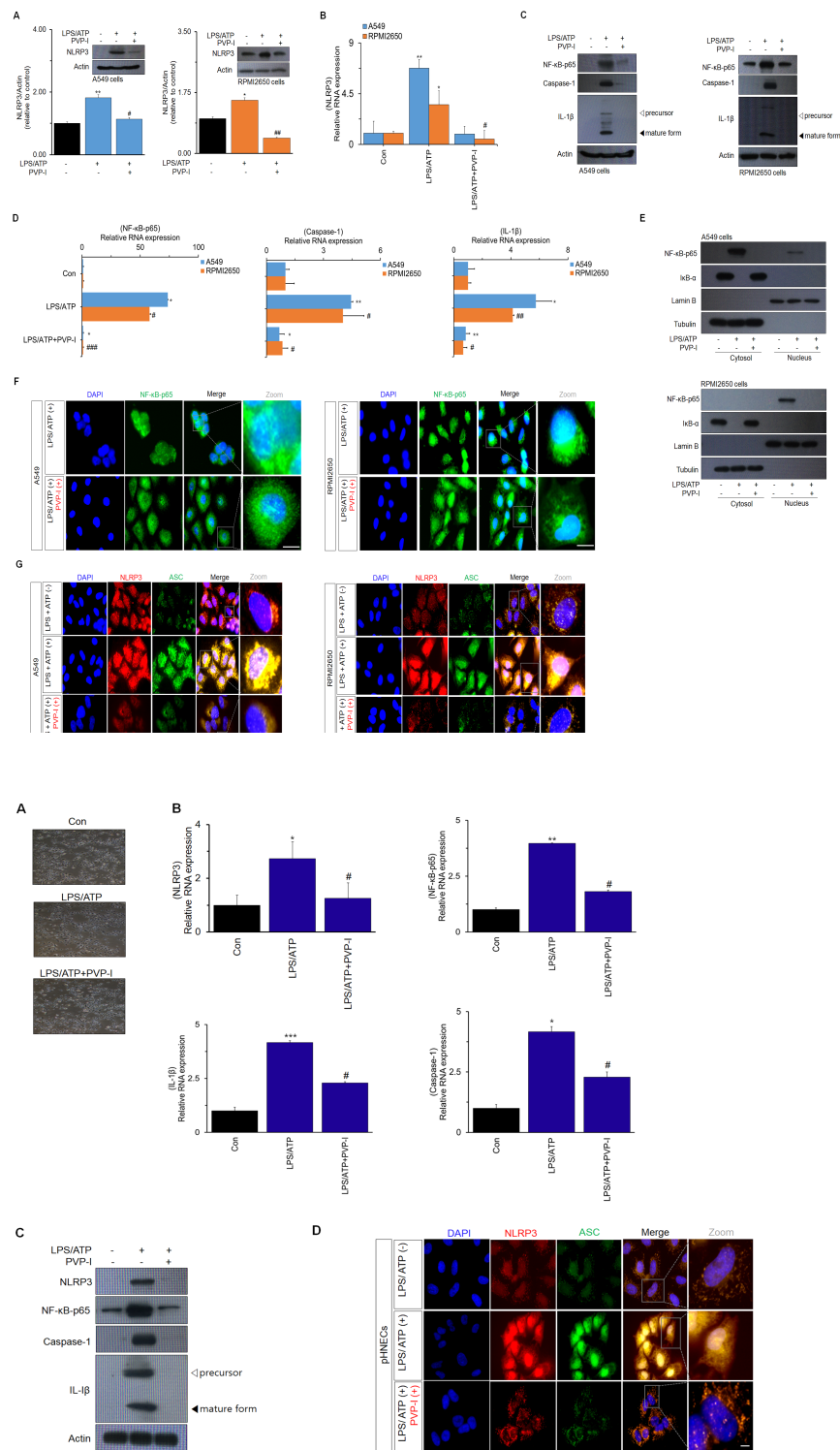
REFERENCE

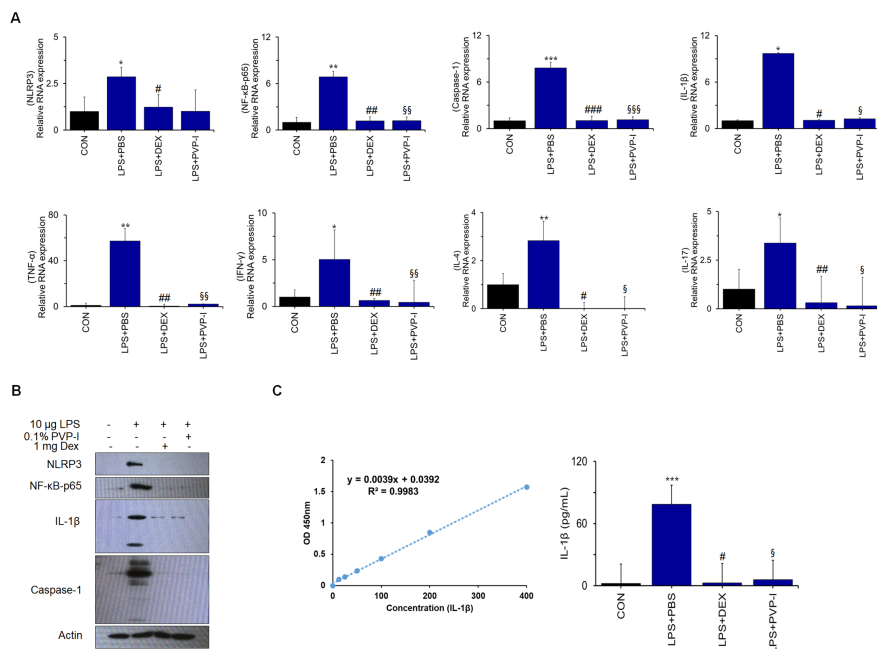
1. Min JY, Nayak JV, Hulse KE, Stevens WW, Raju PA, Huang JH, Suh LA, Van Roey GA, Norton JE, Carter RG, Price CPE, Weibman AR, Rashan AR, Ghosn EE, Patel ZM, Homma T, Conley DB, Welch KC, Shintani-Smith S, Peters AT, Grammer LC 3rd, Harris KE, Kato A, Hwang PH, Kern RC, Herzenberg LA, Schleimer RP, Tan BK. Evidence for altered levels of IgD in the nasal airway mucosa of patients with chronic rhinosinusitis. *J Allergy Clin Immunol* 2017;6:1562-1571
2. Bachert C, Marple B, Hosemann W, Cavaliere C, Wen W, Zhang N. Endotypes of Chronic Rhinosinusitis with Nasal Polyps: Pathology and Possible Therapeutic Implications. *J Allergy Clin Immunol Pract* 2020;8:1514-1519
3. Tomassen P, Vandeplass G, Van Zele Tet al. Inflammatory endotypes of chronic rhinosinusitis based on cluster analysis of biomarkers. *J Allergy Clin Immunol* 2016; 137:1449-1456 e1444

4. Liao B, Liu JX, Li ZY et al. Multidimensional endotypes of chronic rhinosinusitis and their association with treatment outcomes. *Allergy* 2018; 73:1459-1469
5. Van Zele T, Claeys S, Gevaert P et al. Differentiation of chronic sinus diseases by measurement of inflammatory mediators. *Allergy* 2006; 61:1280-1289
6. Van Bruaene N, Perez-Novo CA, Basinski T et al. T-cell regulation in chronic paranasal sinus disease. *J Allergy Clin Immunol* 2008;121:1435-1441
7. Wang X, Zhang N, Bo M et al. Diversity of TH cytokine profiles in patients with chronic rhinosinusitis: A multicenter study in Europe, Asia, and Oceania. *J Allergy Clin Immunol* 2016;138:1344-1353
8. Mahdavinia M, Suh LA, Carter R et al. Increased noneosinophilic nasal polyps in chronic rhinosinusitis in US second-generation Asians suggest genetic regulation of eosinophilia. *J Allergy Clin Immunol* 2015; 135:576-579
9. Wang H, Li ZY, Jiang WX et al. The activation and function of IL-36gamma in neutrophilic inflammation in chronic rhinosinusitis. *J Allergy Clin Immunol* 2018; 141:1646-1658
10. Cao PP, Wang ZC, Schleimer RP, Liu Z. Pathophysiologic mechanisms of chronic rhinosinusitis and their roles in emerging disease endotypes. *Ann Allergy Asthma Immunol* 2019; 122:33-40
11. Wen W, Liu W, Zhang L et al. Increased neutrophilia in nasal polyps reduces the response to oral corticosteroid therapy. *J Allergy Clin Immunol* 2012; 129:1522-1528 e1525
12. Cardell LO, Stjarne P, Jonstam K, Bachert C. Endotypes of chronic rhinosinusitis: Impact on management. *J Allergy Clin Immunol* 2020; 145:752-756
13. Davis BK, Wen H, Ting JP. The inflammasome NLRs in immunity, inflammation, and associated diseases. *Annual review of immunology* 2011; 29:707-735
14. De Nardo D, Latz E. NLRP3 inflammasomes link inflammation and metabolic disease. *Trends in immunology* 2011;32:373-379
15. Martinon F, Burns K, Tschopp J. The inflammasome: a molecular platform triggering activation of inflammatory caspases and processing of proIL-beta. *Molecular cell* 2002; 10:417-426
16. Lima C, Falcao MAP, Andrade-Barros A et al. Natterin an aerolysin-like fish toxin drives IL-1beta-dependent neutrophilic inflammation mediated by caspase-1 and caspase-11 activated by the inflammasome sensor NLRP6. *Int Immunopharmacol* 2020;91:107287
17. Haneklaus M, O'Neill LA. NLRP3 at the interface of metabolism and inflammation. *Immunol Rev* 2015; 265:53-62
18. Lin H, Li Z, Lin D, Zheng C, Zhang W. Role of NLRP3 Inflammasome in Eosinophilic and Non-eosinophilic Chronic Rhinosinusitis with Nasal Polyps. *Inflammation* 2016; 39:2045-2052
19. Wei Y, Zhang J, Wu X et al. Activated pyrin domain containing 3 (NLRP3) inflammasome in neutrophilic chronic rhinosinusitis with nasal polyps (CRSwNP). *J Allergy Clin Immunol* 2020; 145:1002-1005 e1016
20. Messenger S, Goddard PA, Dettmar PW, Maillard JY. Determination of the antibacterial efficacy of several antiseptics tested on skin by an 'ex-vivo' test. *J Med Microbiol* 2001; 50:284-292
21. Rikimaru T, Kondo M, Kondo S, Oizumi K. Efficacy of common antiseptics against mycobacteria. *Int J Tuberc Lung Dis* 2000; 4:570-576
22. Kawana R, Kitamura T, Nakagomi O et al. Inactivation of human viruses by povidone-iodine in comparison with other antiseptics. *Dermatology* 1997;195 Suppl 2:29-35
23. Eggers M. Infectious Disease Management and Control with Povidone Iodine. *Infect Dis Ther* 2019;8:581-593

24. Arakeri G, Brennan PA. Povidone-iodine: an anti-oedematous agent? *Int J Oral Maxillofac Surg* 2011; 40:173-176
25. Wang L, Qin W, Zhou Yet al. Transforming growth factor beta plays an important role in enhancing wound healing by topical application of Povidone-iodine. *Sci Rep* 2017;7:991
26. Panchmatia R, Payandeh J, Al-Salman Ret al. The efficacy of diluted topical povidone-iodine rinses in the management of recalcitrant chronic rhinosinusitis: a prospective cohort study. *Eur Arch Otorhinolaryngol* 2019; 276:3373-3381
27. Wang S, Zhang H, Xi Zet al. Establishment of a mouse model of lipopolysaccharide-induced neutrophilic nasal polyps. *Exp Ther Med* 2017; 14:5275-5282
28. Rombaux P, Collet S, Hamoir Met al. The role of nasal cavity disinfection in the bacteriology of chronic sinusitis. *Rhinology* 2005; 43:125-129
29. Rylander R. Endotoxin in the environment—exposure and effects. *J Endotoxin Res* 2002; 8:241-252
30. Hornung V, Latz E. Critical functions of priming and lysosomal damage for NLRP3 activation. *European journal of immunology* 2010; 40:620-623
31. Guarda G, Zenger M, Yazdi ASet al. Differential expression of NLRP3 among hematopoietic cells. *Journal of immunology (Baltimore, Md : 1950)* 2011;186:2529-2534
32. Lamkanfi M, Dixit VM. Inflammasomes: guardians of cytosolic sanctity. *Immunological reviews* 2009; 227:95-105
33. Tschopp J, Schroder K. NLRP3 inflammasome activation: The convergence of multiple signalling pathways on ROS production?. *Nature reviews Immunology* 2010;10:210-215
34. Ozaki E, Campbell M, Doyle SL. Targeting the NLRP3 inflammasome in chronic inflammatory diseases: current perspectives. *Journal of inflammation research* 2015; 8:15-27
35. Menu P, Vince JE. The NLRP3 inflammasome in health and disease: the good, the bad and the ugly. *Clinical and experimental immunology* 2011; 166:1-15
36. Mason DR, Beck PL, Muruve DA. Nucleotide-binding oligomerization domain-like receptors and inflammasomes in the pathogenesis of non-microbial inflammation and diseases. *Journal of innate immunity* 2012; 4:16-30
37. Hosseinian N, Cho Y, Lockey RF, Kolliputi N. The role of the NLRP3 inflammasome in pulmonary diseases. *Therapeutic advances in respiratory disease* 2015; 9:188-197
38. Simpson JL, Phipps S, Baines KJ, Oreo KM, Gunawardhana L, Gibson PG. Elevated expression of the NLRP3 inflammasome in neutrophilic asthma. *The European respiratory journal* 2014; 43:1067-1076
39. Kelley N, Jeltama D, Duan Y, He Y. The NLRP3 Inflammasome: An Overview of Mechanisms of Activation and Regulation. *int j mol sci* 2019;20:3328
40. Vajjhala PR, Mirams RE, Hill EJM. Multiple binding sites on the pyrin domain of ASC protein allow self-association and interaction with NLRP3 protein. *J Biol Chem* 2012;287:41732-41743
41. Hu H, Li H. Prunetin inhibits lipopolysaccharide-induced inflammatory cytokine production and MUC5AC expression by inactivating the TLR4/MyD88 pathway in human nasal epithelial. *cells Biomed Pharmacother* 2018;106
42. Yang HW, Kim H-J, Park J-H, Shin J-M, Lee H-M. Apigenin alleviates TGF- β 1-induced nasal mucosa remodeling by inhibiting MAPK / NF-kB signaling pathways in chronic rhinosinusitis. *PLoS One* 2018;13:e0201595

43. Li XZ, Zhao SC, Cai XL, Wang YF, Chen J, Ma XF, Zhang H. Differences in expression of YKL-40 and TLR4 in nasal sinus mucosa of chronic sinusitis patients with and without nasal polyps. *J Biol Regul Homeost Agents* 2018; 32:537-543
44. Su Q, Li L, Sun Y, Yang H, Ye Z, Zhao J. Effects of the TLR4/Myd88/NF- κ B Signaling Pathway on NLRP3 Inflammasome in Coronary Microembolization-Induced Myocardial Injury. *Cell Physiol Biochem* 2018;47:1497-1508
45. Jung HJ, Zhang YL, Kim DK, Rhee CS, Kim DY. The Role of NF- κ B in Chronic Rhinosinusitis With Nasal Polyps. *Allergy Asthma Immunol Res* 2019;11:806-817
46. ho J-S, Kim J-A, Park J-H, Park I-H, Han I-H, Lee H-M. Toll-like receptor 4-mediated expression of interleukin-32 via the c-Jun N-terminal kinase/protein kinase B/cyclic adenosine monophosphate response element binding protein pathway in chronic rhinosinusitis with nasal polyps. *Int Forum Allergy Rhinol* 2016; 6:1020-1028
47. Sriwilaijaroen N, Wilairat P, Hiramatsu H, Takahashi T, Suzuki T, Ito M, Ito Y, Tashiro M, Suzuki Y. Mechanisms of the action of povidone-iodine against human and avian influenza A viruses: its effects on hemagglutination and sialidase activities. *Virol J* 2009;6:124
48. Raetz CRH, Whitfield C. Lipopolysaccharide endotoxins. *Annu Rev Biochem* 2002; 71:635-700
49. Bae JS, Kim JH, Kim EH, Mo JH. The Role of IL-17 in a Lipopolysaccharide-Induced Rhinitis Model. *Allergy Asthma Immunol Res* 2017; 9:169-176
50. Pawankar R. Nasal polyposis: an update: editorial review. *Curr Opin Allergy Clin Immunol* 2003;3:1-6
51. Yasir M, Goyal A, Bansal P, Sonthalia S. Corticosteroid Adverse Effects. In: *StatPearls* [Internet]. Treasure Island (FL): StatPearls Publishing; 2020
52. Kalpokas I, Perdigón F, Rivero R, Talmon M, Sartore I, Viñoles C. Effect of a povidone-iodine intrauterine infusion on progesterone levels and endometrial steroid receptor expression in mares. *Acta Vet Scand* 2010;1:653
53. Lin H, Li Z, Lin D, Zheng C, Zhang W. Role of NLRP3 Inflammasome in Eosinophilic and Non-eosinophilic Chronic Rhinosinusitis with Nasal Polyps. *Inflammation* 2016;6:2045-2052
54. Perkins C, Wills-Karp M, Finkelman FD. IL-4 induces IL-13-independent allergic airway inflammation. *J Allergy Clin Immunol* 2006;2:410-9
55. Brightling CE, Chané P, Leigh R, O'Byrne PM, Korn S, She D, May RD, Streicher K, Ranade K, Piper E. Efficacy and safety of tralokinumab in patients with severe uncontrolled asthma: a randomised, double-blind, placebo-controlled, phase 2b trial. *Lancet Respir Med* 2015 9:692-701
56. Alagha K, Bourdin A, Vernisse C, Garulli C, Tummino C, Charriot J, Vachier I, Suehs C, Chané P, Gras D. Goblet cell hyperplasia as a feature of neutrophilic asthma. *Clin Exp Allergy* 2019; 6:781-788
57. Panchmatia R, Payandeh J, Al-Salman R, Kakande E, Habib AR, Mullings W, Javer AR. The efficacy of diluted topical povidone-iodine rinses in the management of recalcitrant chronic rhinosinusitis: a prospective cohort study. *Eur Arch Otorhinolaryngol* 2019;12:3373-3381.





Oligonucleotides			
Gene	5'→	Human	Mouse
NLRP3	Forward	GGACTGAAGCACCTGTTGTGCA	TCACAACTCGCCC AAGGAGGAA
	Reverse	TCCTGAGTCTCCCAAGGCATTC	AAGAGACCACGGCAGAAGCTAG
Caspase-1	Forward	GCTGAGGTTGACATCACAGGCA	GGCACATTCCAGGACTGACTG
	Reverse	TGCTGTCAGAGGTC TTGTGCTC	GCAAGACGTGTACGAGTGGTTG
IL-1β	Forward	CCACAGACCTCCAGGAGAATG	TGGACCTCCAGGATGAGGACA
	Reverse	GTGCAGTTCAGTGATC GTACAGG	GTTATCTCGGAGCCTGTAGTG
NF-κB-p65	Forward	TGAACCGAAACTCTGGCAGCTG	TCC TGTTCTGAGTCTCCATGCAG
	Reverse	CATCAGCTTGC GAAAAGGAGCC	GGTCTCATAGGTCCTTTTGCCG
IL-4	Forward	CCGTAACAGACATCTTTGCTGCC	ATCATCGGCATTTTAACGAGGTC
	Reverse	GAGTGTCCTTCTCATGGTGGCT	ACCTTGGAAGCCC TACAGACGA
IL-17	Forward	CGGACTGTGATGGTCAACCTGA	CAGACTACCTCAACGTTCCAC
	Reverse	GCAC TTTGCCTCCAGATCACA	TCCAGCTTTCCCTCCGCAATTGA
TNF-α	Forward	CTCTTCTGCTGCTGCAC TTTG	GGTGCC TATGCTTCAGCCCTCTT
	Reverse	ATGGGCTACAGGCTTGTCACTC	GCCATAGAATGATGAGAGGGAG
IFN-γ	Forward	GAGTGTGGAGACCATCAAGGAAG	CAGCAACAGCAAGGC GAAAAAGG
	Reverse	TGCTTTGC GTTGACATTCAAGTC	TTTCCGCTTCTGAGGCTGGAT

